Nano Research

Open Access

Review Article

Recent advances in anticancer metallodrugs based on gold complexes and clusters

Xiaoni An and Liang Zhao ✉

The Key Laboratory of Bioorganic Phosphorus Chemistry & Chemical Biology (Ministry of Education), Department of Chemistry, Tsinghua University, Beijing 100084, China

Cite this article: *Nano Research*, **2026**, *19*, 94908509. https://doi.org/10.26599/NR.2026.94908509

ABSTRACT: In the field of metal-based anticancer agents, gold-based drugs have emerged as one of the most promising research directions following platinum-based drugs, owing to their unique physicochemical properties and distinct anticancer mechanisms. This review introduces Au(I) complexes, Au(III) complexes and gold clusters separately, summarizing the recent advances in the anticancer research of gold complexes and gold clusters with well-defined structures. Special emphasis is placed on the ligand design and structure–activity relationships of Au(I) complexes, the synthetic strategies and anticancer mechanisms of Au(III) complexes, as well as the characteristics of gold cluster drugs. Furthermore, the future development directions of gold-based anticancer agents are prospected, including the development of novel targeted ligands, the combination of cancer therapies, and in-depth elucidation of their mechanisms of action.

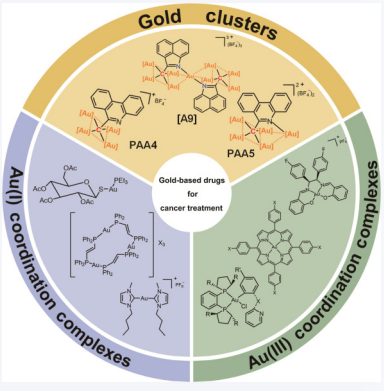

KEYWORDS: Au(I), Au(III), gold clusters, cancer therapy

1 Introduction

Among the diverse array of chemotherapeutic agents, metal-based drugs have garnered substantial attention since the discovery of cisplatin in the 1960s [1]. Cisplatin was approved by the Food and Drug Administration (FDA) in 1978 and became the first metal-based drug for cancer therapy [2]. However, cisplatin has drug resistance and serious toxic side effects in clinical applications, such as nephrotoxicity, ototoxicity and neurotoxicity. These factors significantly limit its therapeutic efficacy [2, 3]. To overcome these limitations, researchers have successively developed second- and third-generation platinum-based drugs, including carboplatin [4], oxaliplatin [5], nedaplatin [6] and lobaplatin [7]. Although these platinum-based drugs play a significant role in the chemotherapy of various solid tumors [8], toxicities and drug resistance remain the main challenges that restrict their clinical utility [9]. For example, cumulative doses of oxaliplatin exceeding 800 mg/m^2 can lead to severe neuropathy, which may persist for more than 2 years after the completion of treatment [10, 11].

To address these challenges, current cancer therapeutic strategies are evolving toward multiple directions. On one hand, researchers are committed to developing novel platinum complexes by introducing diverse bioactive ligands, aiming to improve lipophilicity, enhance targeting specificity, and reduce toxic side effects [12, 13]. On the other hand, given the inherent limitations of platinum-based drugs, research efforts have turned to the development of non-platinum chemotherapeutic agents [14]. Transition metals, such as ruthenium (Ru), copper (Cu), osmium (Os), iridium (Ir), and gold (Au), have attracted attention due to their unique coordination chemistry properties, redox activities, and structural diversity [15], especially gold-based drugs [16]. This is attributed to the similar coordination properties of Au(III) to those of Pt(II). Furthermore, Au(I) possesses a higher reduction potential (1.69 V vs. SHE) than Pt(II) (1.18 V vs. SHE). This indicates that Au(I) is more prone to being reduced to Au(0) in the biological system, which can then be efficiently excreted through the body's metabolic processes. Consequently, Au(I) complexes are less likely to induce systemic toxic side effects, a common limitation associated with Pt(II) complexes.

The medicinal application of gold dates back to 2500 BCE in China [17], where gold-containing formulations were utilized for the treatment of measles and other diseases [18]. Later, in 1895, Robert Koch demonstrated the antibacterial activity of potassium dicyanoaurate ($K[Au(CN)_2]$) [17, 19]. In 1972, Sutton and colleagues first reported the synthesis of 2,3,4,6-tetra-O-acetyl-1-

Received: December 22, 2025; **Revised:** January 26, 2026
Accepted: January 29, 2026

✉Address correspondence to zhaolchem@mail.tsinghua.edu.cn

thio-β-D-glucopyranosato-S-(triethylphosphine) gold (auranofin) [20, 21]. In 1985, auranofin became the first gold complex approved by the FDA for the treatment of rheumatoid arthritis [22–25]. Subsequent studies have illustrated that auranofin exhibits anticancer biological activity in different types of cancer cells [26–34]. However, owing to its high affinity for protein thiol groups, it may undergo inactivation before reaching its target and induce side effects [35, 36]. These findings have stimulated the development of next-generation gold complexes for cancer treatment [22, 37], offering a new direction for the discovery of innovative anticancer agents.

Currently, it has been found that the primary mechanism of action of gold-based drugs is the inhibition of thioredoxin reductase (TrxR) activity, disruption of cellular redox homeostasis, excessive production of reactive oxygen species (ROS), and subsequent induction of cell apoptosis [38]. Among these agents, Au(I)-based drugs are mostly linear coordination complexes, whose activity is regulated by ligands. In contrast, Au(III)-based drugs are four-coordinate complexes and are generally reduced to the more active Au(I) species *in vivo* to exert anticancer effects. Meanwhile, researchers have developed gold cluster drugs with well-defined structures. It is anticipated to achieve better anticancer effects by the unique photophysical properties and size effects of gold clusters. In this review, we summarize the structurally well-defined gold-based drugs reported in recent years and elaborate on their biological activities and mechanisms of action.

2 Au(I) and Au(III) coordination complexes

In coordination complexes, the common oxidation states of gold are Au(I) and Au(III), which drives the investigations into their biomedical applications. The selection of appropriate ligands to combine with Au(I) or Au(III) is critical to the efficacy of gold-based drugs, such as ligands with high stability and favorable biocompatibility [39, 40]. Common ligands used in gold-based drugs include phosphines and N-heterocyclic carbenes (NHCs). Both types of ligands possess strong σ-donating capability, which can increase the electron density of the metal center and significantly enhance the stability of the complexes. Au(I) complexes often perform two-coordinate complexes. Therefore, researchers mainly select and combine different ligands to regulate their bioactivity. In contrast, as to square-planar four-coordinate Au(III) complexes, the primary approach is to promote their reduction to Au(I) species in biological systems and then exert anticancer effects.

In this section, we will summarize the types of ligands and their functions of Au(I) complexes. As for Au(III) complexes, we will focus on the reduction mechanism of Au(III) to Au(I) and their antitumor mechanisms *in vivo*, with a brief mention of synthetic methods.

2.1 Au(I) coordination complexes

In the design and development of anticancer Au(I) drugs, phosphine and NHC ligands play a crucial role. In phosphine ligands, the P atom acts as an electron donor to form a coordination bond with Au(I), regulating the electron cloud density of Au(I) and laying the foundation for its biological activity. Meanwhile, modifying phosphine ligands can also regulate the lipophilicity or hydrophilicity of gold complexes, thereby improving their anticancer potential and optimizing pharmacological properties [41]. Figure 1 and Table 1 show the chemical structures

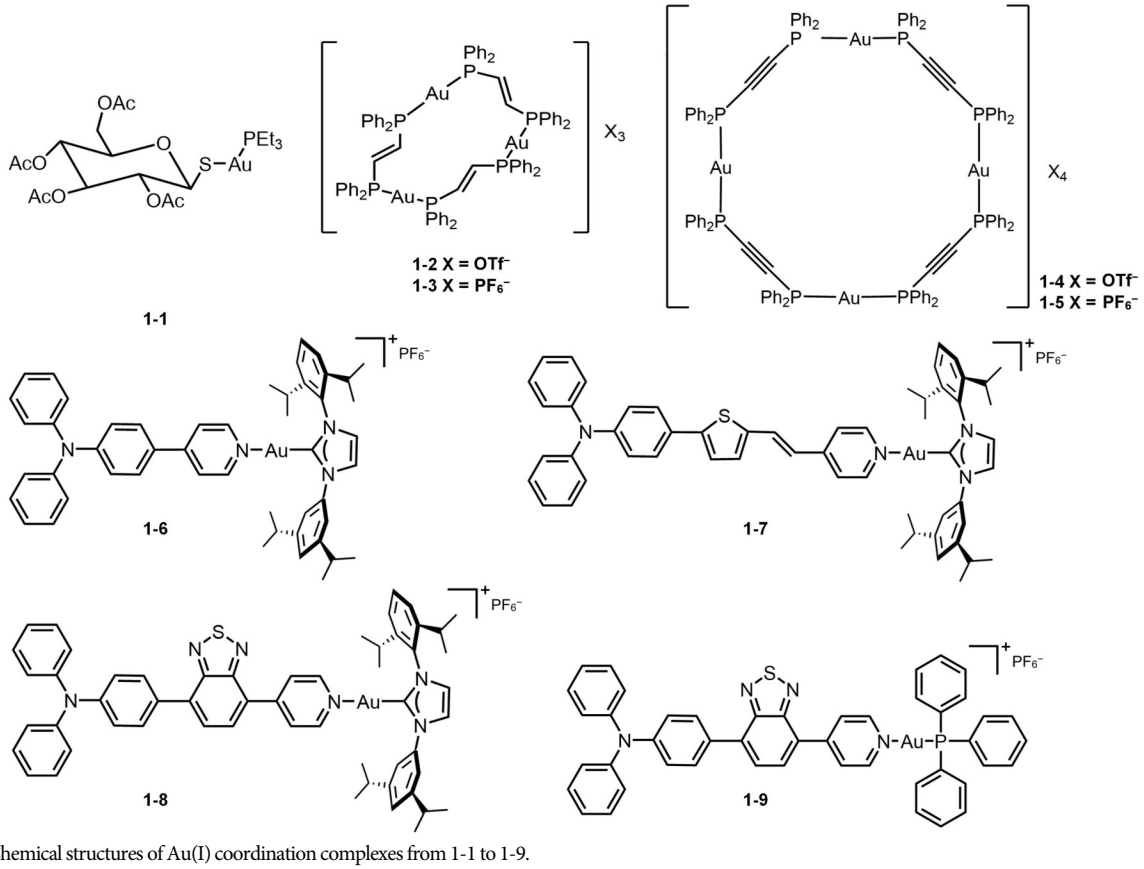

Figure 1 Chemical structures of Au(I) coordination complexes from 1-1 to 1-9.

Table 1 Cytotoxicity of Au(I) coordination complexes from 1-1 to 1-9

Complexes	IC_{50} (μM)[a]	Cell lines	Diseases	References
1-1	1.74 ± 0.32	HepG2	Hepatocellular carcinoma	[51]
	2.24 ± 0.24	SMMC-7721	Hepatocellular carcinoma	
	1.93 ± 0.21	Hep3B	Hepatocellular carcinoma	
	2.09 ± 0.89	Hela	Cervical cancer	
	1.70 ± 0.34	Huh7-LR	Hepatocellular carcinoma	[57]
	2.09 ± 1.25	LO2 (normal hepatocytes)	/	
	3.52 ± 0.62	Hepa1-6	Hepatocellular carcinoma	
	3.10 ± 0.24	MCF-7	Breast cancer	[58]
	1.21 ± 0.09	Ishikawa	Endometrial carcinoma	
	3.61 ± 0.06	HT-29	Colorectal adenocarcinoma	
	2.03 ± 0.59	MDA-MB-231	Breast cancer	[43]
	2.51 ± 0.21	RC-124	Renal cell carcinoma	
	1.58 ± 0.03	MDA-MB-468	Bbreast cancer	
	1.20 ± 0.03	H460	Non-small cell lung cancer	[62]
	4.80 ± 0.01	BT333	Glioblastoma multiforme	
1-2	3.70 ± 0.10	HCT116-p53wt	Colorectal carcinoma	[65]
	2.40 ± 0.50	HCT116-p53wt/OxR	Colorectal carcinoma	
	3.00 ± 0.40	HCT116-p53ko	Colorectal carcinoma	
	3.51 ± 0.30	HCT116-p53ko/OxR	Colorectal carcinoma	
	0.90 ± 0.20	A2780	Ovarian carcinoma	
	3.10 ± 0.40	A2780cis	Ovarian carcinoma	
	1.40 ± 0.4	A375	Cutaneous melanoma	
	6.10 ± 4.60	N87	Gastric adenocarcinoma	
	0.58 ± 0.10	DU145	Prostate adenocarcinoma	
	0.49 ± 0.08	HeLa	Cervical cancer	
	0.36 ± 0.19	MDAMB-231	Breast cancer	
	5.70 ± 1.03	HaCaT (human immortalized keratinocytes)	/	
1-3	4.65 ± 0.64	DU145	Prostate adenocarcinoma	[66]
	1.40 ± 0.25	HeLa	Cervical cancer	
	0.76 ± 0.27	MDAMB-231	Breast cancer	
	18.60 ± 3.70	HaCaT (human immortalized keratinocytes)	/	
1-4	3.92 ± 0.66	DU145	Prostate adenocarcinoma	
	2.89 ± 0.73	HeLa	Cervical cancer	
	1.23 ± 0.15	MDAMB-231	Breast cancer	
	3.60 ± 0.70	HaCaT (human immortalized keratinocytes)	/	
1-5	2.80 ± 0.59	DU145	Prostate adenocarcinoma	
	3.10 ± 0.43	HeLa	Cervical cancer	
	0.91 ± 0.26	MDAMB-231	Breast cancer	
	12.80 ± 2.60	HaCaT (human immortalized keratinocytes)	/	
1-6 (white light irradiation)	4.478–5.271	4T1	Breast cancer	[46]
	5.618–6.218	H292	Non-small cell lung cancer	
	4.627–4.846	HUH7	Hepatocellular carcinoma	
1-7 (white light irradiation)	2.889–3.016	4T1	Breast cancer	
	3.189–3.425	H292	Non-small cell lung cancer	
	3.105–3.297	HUH7	Hepatocellular carcinoma	
1-8 (white light irradiation)	2.202–2.374	4T1	Breast cancer	
	2.002–2.493	H292	Non-small cell lung cancer	
	2.712–3.063	HUH7	Hepatocellular carcinoma	
1-9 (white light irradiation)	1.807–1.943	4T1	Breast cancer	
	1.633–1.836	H292	Non-small cell lung cancer	
	1.869–2.232	HUH7	Hepatocellular carcinoma	

[a] IC_{50} refers to the concentration of the drug that is required to inhibit the growth of the cancerous cell by 50%.

and cytotoxicity of Au(I) coordination complexes from 1-1 to 1-9. Auranofin (complex 1-1) is the earliest gold-based anticancer drug using phosphine ligands [42]. So far, various gold complexes containing phosphine ligands have been confirmed to have cytotoxicity against a variety of cancer cells.

Bhargava et al. focused on the synthesis of trinuclear and tetranuclear Au(I) phosphine complexes with P-Au-P structures. Among them, the core ligands were two types of diphosphine ligands, namely trans-1,2-bis(diphenylphosphino)ethylene (dppen) and bis(diphenylphosphino)acetylene (dppa). Both ligands coordinated with Au(I) centers through a bridging mode, forming cyclic trinuclear complexes $[Au_3(\mu\text{-dppen})_3]X_3$ (complexes 1-2 and 1-3) and tetranuclear complexes $[Au_4(\mu\text{-dppa})_4]X_4$ (complexes 1-4 and 1-5). This coordination mode constructed a stable cyclic polynuclear framework, endowing the complexes with excellent stability. Differences in the bridging groups of ligands influenced the binding affinity of complexes to biological targets. For instance, complex 1-2 with an ethylene bridge group exhibited significantly superior selectivity compared to complex 1-4 with an acetylene bridge group. A comparative analysis between complex 1-2 and complex 1-3 or complex 1-4 and complex 1-5 revealed that trifluoromethanesulfonate anion (OTf^-) display stronger cytotoxicity against most cancer cell lines. Further investigations into the mechanism of cell death have found that these complexes could inhibit the activity of TrxR, induce G_2/M phase cell cycle arrest in tumor cells, suppress cell migration, disrupt F-actin assembly, and trigger cell apoptosis by reducing mitochondrial membrane potential (MMP) and increasing ROS levels. Collectively, these findings confirm that cyclic Au(I) phosphine complexes hold great potential in the research and development of anticancer drugs [66].

Tang et al. designed the ligands of Au(I) complexes to address the existing issues in cancer treatment, such as poor targeting, strong toxic side effects, and drug resistance. Firstly, based on pyridine-containing AIE ligands, they introduced units like thiophene and benzothiazole to gradually enhance the donor (D)–acceptor (A) properties, which solved the aggregation-caused quenching (ACQ) problem of traditional photosensitizers [44, 45]. This endowed the Au(I) complexes with aggregation induced emission (AIE) capability, enabling their application in tumor imaging and photodynamic therapy (PDT) to enhance ROS generation. Secondly, the Au(I)-P bond in phosphine ligands has relatively weak binding affinity, and its coordination with Au(I) can be dynamically regulated in biological systems. Therefore, compared with NHC ligands (complexes 1-6, 1-7, and 1-8), Au(I) in complex 1-9 is more likely to dissociate the triphenylphosphine unit and bind to TrxR in tumor cells. Mechanism research has found that complex 1-9 targeted and inhibited TrxR, efficiently generated ROS, and directly acted on the endoplasmic reticulum (ER), thereby inducing immunogenic cell death (ICD). Ultimately, it realized the integration of chemotherapy, PDT, and immunotherapy, enhancing the antitumor outcome [46].

NHCs are generally defined as heterocyclic compounds containing one carbene carbon and at least one nitrogen atom [47]. In 2004, Berners-Price and his colleagues published the first article on the antitumor properties of gold-NHC complexes [48]. Since then, researchers have gradually recognized that NHC ligands can effectively stabilize the gold center and endow gold complexes with specific biological activities and pharmacological properties. Figure 2 and Table 2 show the chemical structures and cytotoxicity of Au(I) coordination complexes from 2-1 to 2-15.

Liu et al. discovered that 4-methoxy- and 4-fluoro-substituted diaryl Au(I)-NHC complexes exhibited effective anti-cancer activity [50]. Subsequently, they reported a series of halo and pseudohalo Au(I)-NHC complexes (complexes from 2-1 to 2-10) derived from 4,5-diarylimidazol. Among these complexes, NHCs served as the core ligands and formed stable coordination bonds with Au(I). Halide ions or pseudohalide ions bound to Au(I) as weak ligands. Notably, with the increase in the radius of halide ions, the lipophilicity of the complexes increased, and their cytotoxicity was enhanced. Mechanistic studies on complex 2-6, the most active one, revealed that it could inhibit the expression of TrxR, induce the production of ROS, reduce the MMP, arrest the cell cycle at the G2/M phase, and promote cell apoptosis. In *in vivo* experiments, complex 2-6 also ameliorated chronic liver injury, making it a potential candidate for hepatocellular carcinoma (HCC) treatment [51].

Compared with the commonly used imidazolylidene (NHCim) [52, 53], tetrazolylidene (NHCtetr) exhibits a unique substitution effect, which might have rendered the gold center more prone to

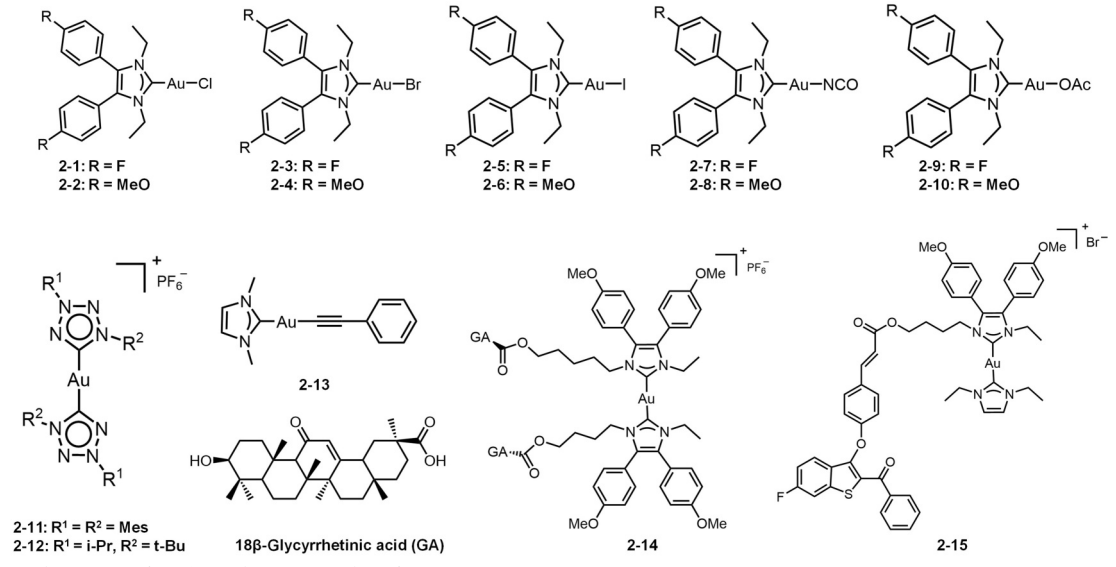

Figure 2 Chemical structures of Au(I) coordination complexes from 2-1 to 2-15.

Table 2 Cytotoxicity of Au(I) coordination complexes from 2-1 to 2-15

Complexes	IC_{50} (μM)	Cell lines	Diseases	References
2-1	> 20	HepG2	Hepatocellular carcinoma	[51]
	16.14 ± 2.79	SMMC-7721	Hepatocellular carcinoma	
	> 20	Hep3B	Hepatocellular carcinoma	
2-2	15.50 ± 1.21	HepG2	Hepatocellular carcinoma	
	7.70 ± 0.41	SMMC-7721	Hepatocellular carcinoma	
	7.90 ± 0.89	Hep3B	Hepatocellular carcinoma	
2-3	3.72 ± 0.15	HepG2	Hepatocellular carcinoma	
	9.41 ± 0.71	SMMC-7721	Hepatocellular carcinoma	
	4.95 ± 0.11	Hep3B	Hepatocellular carcinoma	
2-4	4.44 ± 0.32	HepG2	Hepatocellular carcinoma	
	10.15 ± 1.29	SMMC-7721	Hepatocellular carcinoma	
	4.71 ± 0.22	Hep3B	Hepatocellular carcinoma	
2-5	1.08 ± 0.12	HepG2	Hepatocellular carcinoma	
	1.88 ± 0.15	SMMC-7721	Hepatocellular carcinoma	
	1.05 ± 0.10	Hep3B	Hepatocellular carcinoma	
2-6	0.50 ± 0.02	HepG2	Hepatocellular carcinoma	
	0.92 ± 0.08	SMMC-7721	Hepatocellular carcinoma	
	0.52 ± 0.04	Hep3B	Hepatocellular carcinoma	
2-7	12.10 ± 1.82	HepG2	Hepatocellular carcinoma	
	8.76 ± 0.82	SMMC-7721	Hepatocellular carcinoma	
	7.86 ± 1.22	Hep3B	Hepatocellular carcinoma	
2-8	3.12 ± 0.16	HepG2	Hepatocellular carcinoma	
	3.83 ± 0.18	SMMC-7721	Hepatocellular carcinoma	
	2.41 ± 0.31	Hep3B	Hepatocellular carcinoma	
2-9	1.22 ± 0.11	HepG2	Hepatocellular carcinoma	
	2.47 ± 0.24	SMMC-7721	Hepatocellular carcinoma	
	1.21 ± 0.11	Hep3B	Hepatocellular carcinoma	
2-10	0.71 ± 0.05	HepG2	Hepatocellular carcinoma	
	1.07 ± 0.09	SMMC-7721	Hepatocellular carcinoma	
	0.77 ± 0.08	Hep3B	Hepatocellular carcinoma	
2-11	0.16	K562	Chronic myelogenous leukemia	[54]
	0.14	NiWi-Dau	Glioblastoma multiforme	
	0.03	BJAB	Burkitt lymphoma	
	0.013	BiBo	Glioblastoma multiforme	
	0.014	Nalm-6	Acute lymphoblastic leukemia	
2-12	0.08	LiKa	Glioblastoma multiforme	
	0.017	Nalm-6	Acute lymphoblastic leukemia	
2-13	63.30 ± 1.10	A549	Non-small cell lung cancer	[55]
	70.60 ± 0.70	HepG2	Hepatocellular carcinoma	
	54.30 ± 0.20	MCF-7	Breast cancer	
	52.40 ± 0.20	U87	glioblastoma multiforme	
	3.86 ± 1.11	Hela	Cervical cancer	
2-14	1.34 ± 0.22	Huh7-LR	Hepatocellular carcinoma	[88]
	3.49 ± 0.89	LO2 (normal hepatocytes)	/	
	0.49 ± 0.14	Hepa1-6	Hepatocellular carcinoma	
	1.59 ± 0.43	Hep3B	hepatocellular carcinoma	
2-15	2.37 ± 0.12	HepG2	Hepatocellular carcinoma	[58]
	1.05 ± 0.15	MCF-7	Breast cancer	
	0.45 ± 0.12	Ishikawa	Endometrial carcinoma	

interacting with enzymes and thus favored its application in pharmaceuticals. Aram Prokop et al. reported a new class of 1,3-disubs tituted Au(I) bis-tetrazolylidene complexes targeting leukemia cells. The four nitrogen atoms in the NHCtetr exhibited a strong σ-donating effect to stabilize the Au(I) center and prevent its non-specific binding to glutathione (GSH). Meanwhile, the type of substituents on NHCtetr could be modified to regulate the lipophilicity and functional characteristics. For instance, complex 2-11 exhibited good lipophilicity, which facilitated its selective enrichment in mitochondria and then generated ROS and disrupted the cellular redox balance. More importantly, complex 2-11 could regulate the BCL-2 family proteins, thereby inducing cell apoptosis. However, all experiments in this study were conducted *in vitro* at present [54].

In order to address the challenge of controllably delivering active Au(I) to the target site, Zou et al. reported a novel bioorthogonal activation strategy. The bioactivity of complex 2-13 was conditionally activated via Pd(II)-triggered transmetalation in *in vitro* cellular systems and zebrafish models. The core of this strategy lay in the preliminary synthesis of Au(I) complexes bearing two strong ligands, which did not induce active reactions upon entering cells. Subsequently, Pd(II) complexes were added, initiating a transmetallation reaction that led to the formation of labile NHC–Au(I) species. After the cleavage of the labile bonds in this species, Au(I) was exposed, which could inhibit the activity of TrxR and the proliferation of cancer cells. Additionally, it could disrupt vascular structures and suppress angiogenesis in zebrafish models. Furthermore, if the Pd(II) complex was functionally modified with RGD, the labile NHC–Au(I) species could specifically bind to integrin receptors that are highly expressed on the surface of cancer cells, thereby providing a novel avenue for precise tumor therapy [55].

To achieve higher targeting efficiency of Au(I) complexes toward cancer cells, modifications are performed on ligands in several studies to enable their specific binding to cancer cells. For instance, in order to target HCC cells more effectively, Liu et al. designed a series of NHC-Au(I) complexes containing 18β-glycyrrhetinic acid (GA). GA possesses numerous binding sites in HCC cells, such as the glycyrrhetinic acid receptor (GA-R) [56]. All these complexes shared an identical NHC ligand to stabilize Au(I), while the ligand at the other end varied, including Cl ligands, NHC ligands, and PPh_3 ligands. Researchers revealed that the cytotoxicity of different ligands in HCC cells followed the order: NHC > PPh_3 > Cl. The proposed mechanism was that the coordination between Cl or PPh_3 ligands and Au(I) was relatively weak, which might lead to inactivation of the complexes before they reached the target sites. In contrast, NHC ligands exhibited superior ability to stabilize Au(I), ensuring the complexes were selectively taken up by HCC cells in and exerted effects intracellularly. Mechanistic studies were conducted using complex 2-14, which showed favorable antitumor activity. It was found that complex 2-14 inhibited TrxR activity, increased the level of ROS, and triggered redox homeostasis disorder. This further mediated mitochondrial dysfunction and endoplasmic reticulum stress (ERS), promoting the release of damage-associated molecular patterns (DAMPs) from HCC cells and ultimately inducing ICD. This study provided a novel strategy for the chemoimmunotherapy of HCC [57].

Following the same idea, Liu et al. conjugated NHC-Au(I) with G1T48 (NCT03455270), a clinical selective estrogen receptor degrader (SERD) candidate, for the treatment of estrogen receptor (ER)-positive breast cancer. Complex 2-15 achieved dual targeting of ER and TrxR, thereby providing a novel direction for the development of drugs against ER-positive breast cancer [58].

From the above examples, it can be observed that the two ligands of most Au(I) complexes interact with each other and have different functions. One side of the ligand has a strong binding force and is used to stabilize Au(I). While the other side has a weak binding force and dissociates in specific environments, allowing Au(I) to be exposed and interact with biological molecules. This ligand design principle is analogous to the hemilabile ligand reported in the literature [59], which contributes to maintaining the stability of Au(I) complexes during blood circulation, reducing non-specific toxicity, and moderately enhancing their targeting capability. In addition, Fig. 3 shows the predicted binding poses of (NHC)Au^+ of complex 3-1 to human TrxR [39, 43]. Table 3 shows the cytotoxicity of Au(I) coordination complex 3-1.

Au(I) complexes feature relatively simple synthesis and well-defined structures with facile modifiability. Furthermore, owing to their distinct mechanism of action compared with platinum-based drugs, they exhibit promising potential for the treatment of cancers resistant to cisplatin. However, the stability of Au(I) complexes in intricate biological microenvironments remains a formidable challenge.

2.2 Au(III) coordination complexes

Most Au(III) complexes exhibit poor stability and are easily

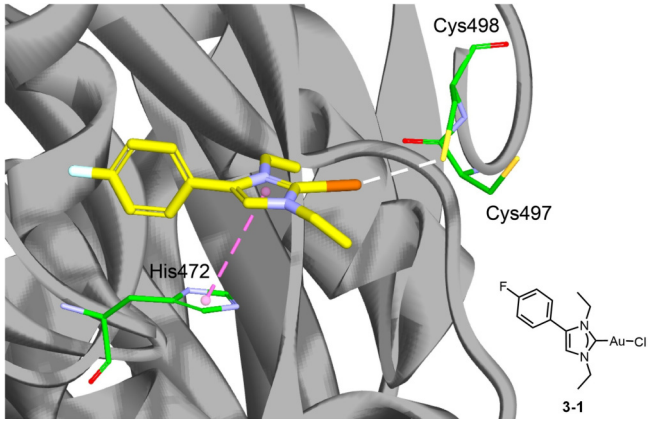

Figure 3 The predicted binding poses of (NHC)Au^+ in the binding pocket of a human TrxR (PDB code 2J3N [49]). Reproduced with permission from Ref. [39], © Wiley Periodicals LLC 2024.

Table 3 Cytotoxicity of Au(I) coordination complex 3-1

Complex	IC_{50} (μM)	Cell lines	Diseases	Reference
3-1 (in DMSO)	9.24 ± 0.70	HT-29	Colorectal adenocarcinoma	[43]
	6.97 ± 0.25	MCF-7	Breast cancer	
	8.22 ± 1.19	MDA-MB-231	Breast cancer	
	8.52 ± 0.76	RC-124	Renal cell carcinoma	

reduced to Au(I) by reductive species such as GSH in biological environments, typically acting as Au(I) prodrugs. In addition, Au(III) complexes are capable of directly interacting with the DNA of cancer cells to induce apoptosis. They can also reduce the MMP, impair mitochondrial function, trigger excessive generation of ROS to elicit oxidative stress damage, and ultimately induce cancer cell apoptosis, thereby achieving anticancer efficacy. In the following sections, we briefly summarize the synthetic strategies of Au(III) complexes, with a primary focus on the reductive transformation of Au(III) to Au(I) in biological systems and its anticancer mechanisms. Figures 4 and 5, as well as Tables 4 and 5, show the chemical structures and cytotoxicity of some Au(I/III) coordination complexes.

Chiral Au(III) complexes have exerted significant impacts on fields such as materials science and asymmetric catalysis [60, 61], yet their application in the anticancer field remains insufficiently explored. Awuah et al. developed a series of chiral Au(III) complexes, [C^N]Au(III)Cl(R-DuPhos) (complexes from 4-1 to 4-7), via the coordination of arylpyridine Au(III) dichloride with chiral diphosphine ligands. By incubating complex 4-2 with L-GSH under simulated physiological conditions *in vitro*, the researchers demonstrated that GSH, acting as a biological reducing agent, reduced Au(III) in the complex to the more stable Au(I) species. The investigations of mechanism revealed that complex 4-2 blocked cellular energy supply by inhibiting the oxygen consumption rate (OCR) of mitochondria, reduced the MMP, disrupted mitochondrial structure and function, and induced excessive ROS production to trigger oxidative stress damage, ultimately exerting cytotoxic effects. Notably, the two isomers of complex 4-7 exhibited a difference of 2 to 4 times in their effects on cytotoxicity. This phenomenon suggested that the chiral center may interact with specific chiral targets within cells, thereby enhancing the targeting ability of the drug. This targeting characteristic is difficult to achieve with achiral gold-based complexes. In conclusion, this study confirms that such chiral Au(III) complexes hold promising potential as next-generation anticancer agents [62].

In the research of NHC-Au(III) compounds, the distribution of the compound after administration and the assessment of its metabolic process of converting into Au(I) substances are important scientific challenges that have not yet been completely resolved to this day. Consequently, Salassa et al. investigated the potential of NHC-Au(III) complexes as anticancer prodrugs through a ^{124}I radiolabeling strategy. They also tracked the *in vivo* biodistribution and metabolic processes of NHC-Au(III) complexes by combining positron emission tomography (PET) and ex vivo analyses. The core strategy for synthesis was the direct oxidation of previously reported complexes 4-8 and 4-9 [63, 64] using radioactive I_2. In *in vitro* experiments, they found that the anticancer mechanisms of complexes 4-8 and 4-10 were similar. Furthermore, ascorbic acid, a strong reducing agent, could significantly enhance the activity of complex 4-10. This directly confirmed that the reduction of Au(III) to Au(I) was the key to exerting anticancer activity. This radiolabeling method provides a new approach for the study of mechanism of action of metal-based drugs [65].

Au(III) complexes can not only act as prodrugs of Au(I), but can also target cancer cells directly. Bertrand et al. reported eight pairs of hemilabile biphenyl NHC-Au(III) complexes, based on the previously mentioned hemilabile ligand concept. Each pair includes neutral open complexes of general formula [(C^C)Au(NHC^het)Cl] (complexes from 4-12a to 4-19a) and chelated cationic complexes of general formula [(C^C)Au(NHC^het)]PF_6 (complexes from 4-12b to 4-19b). The core step of the synthesis process is to use the (2-pyridyl) azolium salts (imidazolium, benzimidazolium, and pyridoimidazolium salts) reported in previous literature [67] as pro-ligands to react with silver oxide, resulting in the formation of silver carbene complexes. Subsequently, the bisphenyl-Au(III) dimeric precursor $[Au]_2$ [89] was added to carry out a transmetallation reaction, and complexes from 4-12a to 4-19a were obtained after the reaction. Afterwards, complexes from 4-12a to 4-19a were respectively used as raw materials to react with $AgPF_6$, leading to the acquisition of cationic complexes (complexes from 4-12b to 4-19b). Researchers found that Cl^- was an unstable ligand that tended to dissociate, thereby exposing Au(III) to exert its function. Mechanistic studies were conducted using BGC19b, the complex with relatively high cytotoxicity. Researchers discovered that it could form stable adducts with cysteine, interfere with the activity of thiol-dependent enzymes or signaling pathways in cells, and disrupt normal cellular physiological functions. Meanwhile, complex 4-19b could impair mitochondrial function, and activate caspase 3/7 to trigger cell apoptosis. This study provided a new method for the development of organogold(III) complexes [59].

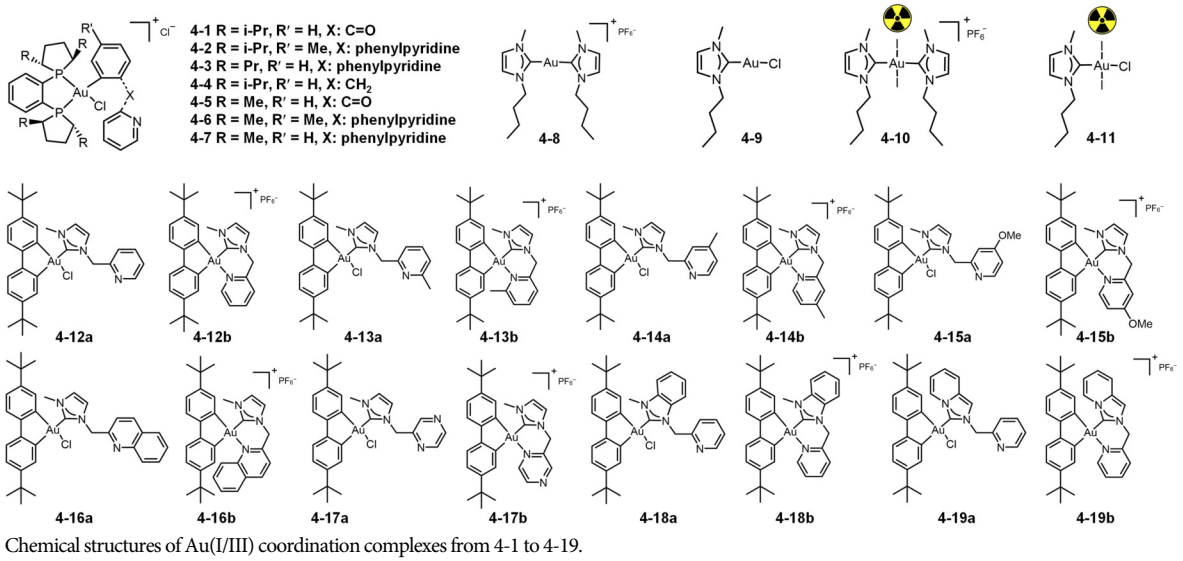

Figure 4 Chemical structures of Au(I/III) coordination complexes from 4-1 to 4-19.

Table 4 Cytotoxicity of some Au(I/III) coordination complexes

Complexes	IC_{50} (μM)	Cell lines	Diseases	References
4-1	1.74 ± 0.36	MDA-MB-468	Breast cancer	[62]
	1.10 ± 0.15	MDA-MB-231	Breast cancer	
	0.48 ± 0.20	H460	Non-small cell lung cancer	
	4.43 ± 0.07	BT333	Glioblastoma multiforme	
4-2	1.30 ± 0.35	MDA-MB-468	Breast cancer	
	1.44 ± 0.15	MDA-MB-231	Breast cancer	
	2.75 ± 0.16	H460	Non-small cell Lung cancer	
	2.95 ± 0.04	BT333	Glioblastoma multiforme	
4-3	5.01 ± 0.35	MDA-MB-468	Breast cancer	
	4.33 ± 0.14	MDA-MB-231	Breast cancer	
	11.48 ± 0.16	H460	Non-small cell lung cancer	
	4.57 ± 0.069	BT333	Glioblastoma multiforme	
4-4	1.07 ± 0.36	MDA-MB-468	Breast cancer	
	1.28 ± 0.16	MDA-MB-231	Breast cancer	
	0.59 ± 0.15	H460	Non-small cell lung cancer	
	2.14 ± 0.09	BT333	Glioblastoma multiforme	
4-5	1.62 ± 0.06	MDA-MB-468	Breast cancer	
	2.19 ± 0.06	MDA-MB-231	Breast cancer	
	2.29 ± 0.06	H460	Non-small cell lung cancer	
	0.219 ± 0.02	BT333	Glioblastoma multiforme	
4-6	3.16 ± 0.07	MDA-MB-468	Breast cancer	
	1.51 ± 0.10	MDA-MB-231	Breast cancer	
	5.75 ± 0.10	H460	Non-small cell lung cancer	
	0.62 ± 0.014	BT333	Glioblastoma multiforme	
4-7	1.18 ± 0.05	MDA-MB-468	Breast cancer	
	0.46 ± 0.06	MDA-MB-231	Breast cancer	
	1.00 ± 0.007	H460	Non-small cell lung cancer	
	0.095 ± 0.12	BT333	Glioblastoma multiforme	
4-8	4.00 ± 0.30	HCT116-p53wt	Colorectal carcinoma	[65]
	1.40 ± 0.60	HCT116-p53wt/OxR	Colorectal carcinoma	
	1.80 ± 0.10	HCT116-p53ko	Colorectal carcinoma	
	>10	HCT116-p53ko/OxR	Colorectal carcinoma	
	2.00 ± 0.40	A2780	Ovarian carcinoma	
	1.00 ± 0.50	A2780cis	Ovarian carcinoma	
	1.50 ± 0.50	MCF-7	Breast cancer	
	1.70 ± 0.40	A375	Cutaneous melanoma	
	5.30 ± 2.40	N87	Gastric adenocarcinoma	
4-10	2.00 ± 0.10	HCT116-p53wt	Colorectal carcinoma	
	1.30 ± 0.50	HCT116-p53wt/OxR	Colorectal carcinoma	
	2.40 ± 0.70	HCT116-p53ko	Colorectal carcinoma	
	> 10	HCT116-p53ko/OxR	Colorectal carcinoma	
	1.80 ± 0.60	A2780	Ovarian carcinoma	
	0.90 ± 0.60	A2780cis	Ovarian carcinoma	
	2.70 ± 0.10	MCF-7	Breast cancer	
	1.80 ± 0.50	A375	Cutaneous melanoma	
	6.20 ± 4.70	N87	Gastric adenocarcinoma	
4-12b	1.80 ± 0.10	HeLa	Cervical cancer	[59]
	1.80 ± 0.10	Huh-7	Hepatocellular carcinoma	
	2.90 ± 0.10	MDA-MB-231	Breast cancer	
	1.20 ± 0.30	MCF-10 A (human normal mammary epithelial)	/	
4-18b	2.80 ± 0.70	HeLa	Cervical cancer	
	2.50 ± 0.40	Huh-7	Hepatocellular carcinoma	
	4.40 ± 0.80	MDA-MB-231	Breast cancer	
	2.80 ± 0.50	MCF-10 A (human normal mammary epithelial)	/	
4-19b	1.80 ± 0.60	HeLa	Cervical cancer	
	1.40 ± 0.10	Huh-7	Hepatocellular carcinoma	
	2.00 ± 0.10	MDA-MB-231	Breast cancer	
	1.60 ± 0.40	MCF-10 A (human normal mammary epithelial)	/	

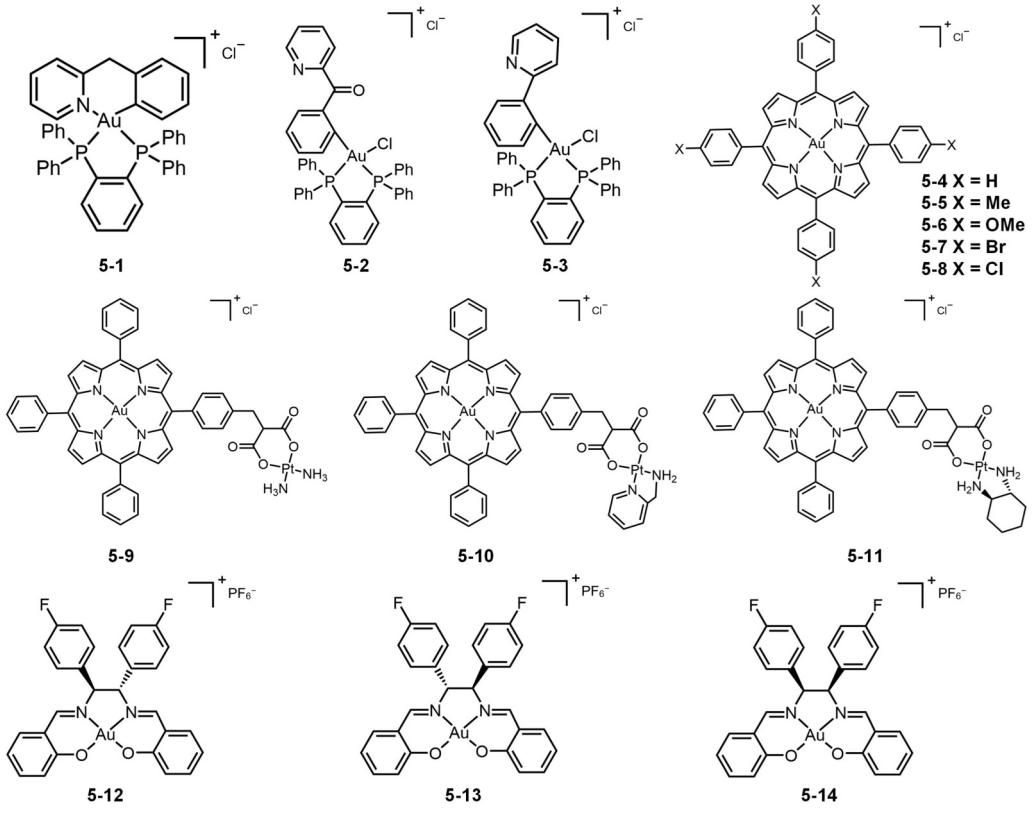

Figure 5 Chemical structures of Au(III) coordination complexes from 5-1 to 5-14.

Table 5 Cytotoxicity of Au(III) coordination complexes from 5-4 to 5-14

Complexes	IC_{50} (μM)	Cell lines	Diseases	References
	0.73 ± 0.02	HL-60	Acute promyelocytic leukemia	
	0.34 ± 0.02	HepG2	Hepatocellular carcinoma	
5-4	0.11 ± 0.02	SUNE1	Nasopharyngeal carcinoma	
	0.28 ± 0.02	Hela	Cervical cancer	
	0.17 ± 0.02	CNE1	Nasopharyngeal carcinoma	
	1.53 ± 0.03	HL-60	Acute promyelocytic leukemia	
	1.11 ± 0.03	HepG2	Hepatocellular carcinoma	
5-5	1.09 ± 0.05	SUNE1	Nasopharyngeal carcinoma	
	0.52 ± 0.02	Hela	Cervical cancer	
	0.99 ± 0.03	CNE1	Nasopharyngeal carcinoma	
	0.88 ± 0.02	HL-60	Acute promyelocytic leukemia	
	0.76 ± 0.05	HepG2	Hepatocellular carcinoma	
5-6	0.68 ± 0.03	SUNE1	Nasopharyngeal carcinoma	[70]
	0.66 ± 0.04	Hela	Cervical cancer	
	0.77 ± 0.03	CNE1	Nasopharyngeal carcinoma	
	1.12 ± 0.09	HL-60	Acute promyelocytic leukemia	
	1.21 ± 0.12	HepG2	Hepatocellular carcinoma	
5-7	0.74 ± 0.08	SUNE1	Nasopharyngeal carcinoma	
	0.89 ± 0.11	Hela	Cervical cancer	
	0.98 ± 0.04	CNE1	Nasopharyngeal carcinoma	
	0.87 ± 0.03	HL-60	Acute promyelocytic leukemia	
	0.92 ± 0.02	HepG2	Hepatocellular carcinoma	
5-8	0.34 ± 0.02	SUNE1	Nasopharyngeal carcinoma	
	0.69 ± 0.02	Hela	Cervical cancer	
	0.41 ± 0.06	CNE1	Nasopharyngeal carcinoma	

(Continued)

Complexes	IC_{50} (μM)	Cell lines	Diseases	References
5-9	2.36	MCF-7	Breast cancer	[72]
	2.23	FS-68	Healthy fibroblasts	
5-10	1.34	MCF-7	Breast cancer	
	2.41	FS-68	Healthy fibroblasts	
5-11	0.90	MCF-7	Breast cancer	
	1.70	FS-68	Healthy fibroblasts	
5-12	5.40 ± 0.99	HepG2	Hepatocellular carcinoma	[73]
	10.05 ± 1.19	SMMC-7721	Hepatocellular carcinoma	
	10.89 ± 1.26	Hep3B	Hepatocellular carcinoma	
5-13	7.50 ± 0.77	HepG2	Hepatocellular carcinoma	
	10.17 ± 1.88	SMMC-7721	Hepatocellular carcinoma	
	12.01 ± 1.82	Hep3B	Hepatocellular carcinoma	
5-14	10.29 ± 1.14	HepG2	Hepatocellular carcinoma	
	8.25 ± 1.29	SMMC-7721	Hepatocellular carcinoma	
	9.03 ± 1.26	Hep3B	Hepatocellular carcinoma	

To prevent the reduction of Au(III) to Au(I), Awuah et al. introduced ligands such as 1,2-bis(diphenylphosphino) benzene and adopted a cyclometalation strategy to stabilize the Au(III) center, thereby synthesizing a series of novel Au(III)-bisphosphine complexes. The key step of the synthesis involved the reaction of $HAuCl_4$ with the corresponding benzyl or benzoylpyridine ligand, yielding a cyclometalated Au(III) intermediate with considerable stability to prevent premature deactivation. In *in vitro* experiments, complexes 5-1, 5-2 and 5-3 exerted potent cytotoxic effects against various cancer cell lines. In particular, complex 5-3 was selectively accumulated in the mitochondria of cancer cells, triggering oxidative stress and inducing apoptosis, providing a novel strategy for the development of anticancer agents [68].

Porphyrin is a naturally occurring tetrapyrrole macrocyclic ligand. Its planar structure, strong coordination ability, and ease of functionalization make it an ideal choice for the design of metal complexes. Researchers aim to develop novel drugs with higher stability, selectivity, and anticancer activity by combining Au(III) with porphyrin ligands [69].

In 2003, Sun et al. developed a series of anticancer Au(III) porphyrin complexes (complexes from 5-4 to 5-8). These complexes were synthesized via the reaction of tetraphenylporphyrin (TPP) with an excess of $KAuCl_4$ in glacial acetic acid [69]. The chelation of porphyrin to Au(III) within the complexes endowed them with high stability. For instance, when complex 5-4 was mixed with GSH, no oxidation of GSH to form glutathione disulfide (GSSG) was observed. In cytotoxicity assays, complex 5-4 exhibited the most prominent anticancer activity, with an IC_{50} range of 0.1–0.8 μM. Further mechanistic studies revealed that this class of complexes could induce cancer cell death through an apoptotic pathway by binding to DNA, which provided a crucial direction for the development of Au(III) porphyrin-based anticancer drugs [70].

PDT has attracted extensive attention in the field of tumor treatment due to its advantages such as low cost, minimal invasiveness, and extremely few side effects compared with traditional chemotherapy [71]. Kobeissi et al. synthesized three novel dyads with Au(III) porphyrin and platinum diamine complex connected through a malonate bridging group for the first time (complexes from 5-9 to 5-11), which could achieve PDT. In *in vitro* experiments, complex 5-11 showed the strongest cytotoxicity and the Au(III)/Pt(II) dyads exhibited 2.0–5.6 fold higher toxicity than the corresponding platinum complexes. Further mechanism studies revealed that these complexes could generate ROS through the type I mechanism in PDT. Moreover, light irradiation only increased the death of cancer cells without affecting healthy cells, which demonstrated that this dyad system possessed both chemical toxicity and PDT specificity in anticancer applications [72].

Schiff bases are a class of organic compounds containing imine functional groups, usually prepared by the condensation reaction of aldehydes or ketones with primary amines. Schiff base ligands can form stable chelates with Au(III) and possess strong coordination ability. They also have diverse and modifiable structures.

To develop gold-based drugs with enhanced stability for targeting TrxR in the treatment of HCC, Liu et al. synthesized a series of Au(III) complexes (complexes from 5-12 to 5-14) bearing Schiff base ligands. These compounds were primarily prepared through the reaction of the corresponding Schiff base ligands with $NaAuCl_4{\cdot}2H_2O$. Mechanistic studies on complex 5-12 with the highest activity revealed that its Au(III) center targeted TrxR and inhibited its activity, leading to an increase in the level of ROS and the activation of ERS, ultimately resulting in the apoptosis of cancer cells. In *in vivo* experiments, complex 5-12 significantly ameliorated liver injury in mice by downregulating the expression of TrxR and the levels of inflammatory factors, thereby emerging as a potential candidate drug for HCC therapy [73].

From the above examples, it can be observed that there are mainly two synthetic methods for Au(III) complexes. One involves the direct reaction of Au(III) compounds (such as $HAuCl_4$, $NaAuCl_4{\cdot}2H_2O$, $KAuCl_4$) with ligands, while the other is the oxidation of Au(I) complexes (such as NHC-Au(I)) to obtain the corresponding Au(III) complexes.

Apart from the development of ligands for Au(I/III) complexes via traditional organic synthesis methods, some researchers derive novel ligand structures from natural products. Figure 6 and Table 6 show the chemical structures and cytotoxicity of some Au(I/III) coordination complexes. For instance, Tamm et al. selected the marine natural product 1,3-dimethylimidazolium-4-carboxylate

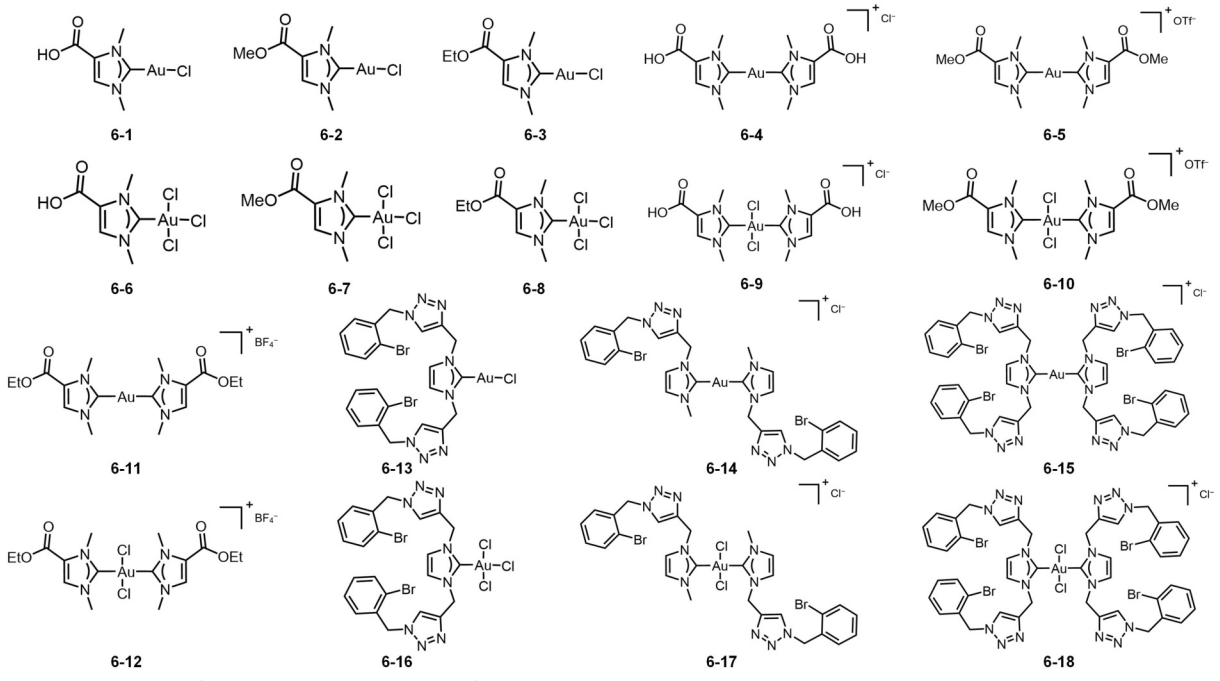

Figure 6 Chemical structures of Au(I/III) coordination complexes from 6-1 to 6-18.

(norzooanemonin) for their research. This compound enabled the introduction of carboxyl groups onto NHC ligands, thereby achieving a novel functionalization of NHC ligands. They initially synthesized the complexes 6-1 and 6-4, but these complexes exhibited high polarity, which hindered cellular uptake and thereby reduced their cytotoxicity against cancer cells [74]. To enhance lipophilicity, they further subjected complexes 6-1 and 6-4 to esterification, and employed $PhICl_2$ as an oxidant to oxidize Au(I) to Au(III). Eventually, complexes from 6-1 to 6-12 were successfully prepared. In cytotoxicity assays, researchers found that the esterification modification of complexes could significantly enhance their cellular uptake and antiproliferative activity. Among these complexes, compared with monocarbene complexes, the dicarbene complexes (6-5, 6-10, 6-11, 6-12) showed superior antiproliferative activity. Moreover, the activities of Au(I) complexes were comparable to those of Au(III) complexes [75]. Nevertheless, this study did not further conduct research on the mechanism by which these compounds act on cancer cells.

In addition to studying the effects of a single type of NHC ligand separately, some researchers are also attempting to combine various types of NHC ligands to observe their anti-cancer effects. For example, Baker et al. synthesized a new triazole-functionalized imidazole salt through the Click reaction, and subsequently prepared NHC-Au(I) and NHC-Au(III) complexes. Among these complexes, the Au(I) complexes could be oxidized to Au(III) complexes using $SOCl_2$. In *in vitro* experiments, researchers selected cisplatin-resistant ovarian cancer cells (OVCAR-8 cells) to perform cytotoxicity assays. The results demonstrated that complexes from 6-13 to 6-18 possessed significant activity, with an IC_{50} value of less than 15 μM [76]. However, this study did not further carry out experimental verification to investigate the mechanism by which these compounds act on ovarian cancer cells.

Au(III) complexes typically adopt a square-planar geometry, which confers greater flexibility for structural modification and ligand selection, and they exhibit potent antiproliferative activity against a broad spectrum of cancer cell lines. However, these complexes are prone to reduction or decomposition in complex biological microenvironments, resulting in poor stability.

3 Gold clusters

Owing to the strong metallic interactions between gold atoms, they tend to spontaneously form nanoscale aggregates. Synthetic methods for these gold-based aggregates have been well-established. gold nanoparticles (AuNPs) possess a particle size ranging from 1 to 100 nm and exhibit the enhanced permeability and retention (EPR) effect as well as excellent optical properties, which can be applied in fields such as PDT and photothermal therapy (PTT) [77–79]. Moreover, the conjugation of AuNPs with antibodies, peptides, or proteins can enhance their targeting capability [80, 81]. These superior characteristics have propelled the development of AuNPs in the field of cancer therapy. However, to gain a deeper insight into the mechanisms underlying the pharmacological actions of these agents, researchers have successively developed gold cluster drugs with well-defined structures to advance relevant research. Furthermore, compared with AuNPs, gold clusters have smaller sizes, which allow them to cross biological barriers more readily, thereby reaching deep tumor regions and intracellular targets more efficiently. This also enables them to be metabolized by the kidney and excreted from the body [82], thus reducing the risk of nephrotoxicity induced by long-term accumulation.

Gold clusters refer to compounds composed of three or more gold atoms and their ligands. Different from gold coordination complexes, gold clusters contain more gold atoms, endowing them with excellent optical properties [83]. For instance, under near-infrared (NIR) irradiation, gold clusters can efficiently absorb light energy and convert it into thermal energy, achieving selective killing of tumor cells [84]. In addition, gold clusters can also act as photosensitizers to generate ROS upon light irradiation, inducing tumor cell apoptosis [85]. These properties enable gold clusters to be used in PTT and PDT, reducing damage to normal human cells. Meanwhile, due to their good X-ray absorption capacity, gold

Table 6 Cytotoxicity of some Au(I/III) coordination complexes

Complexes	IC_{50} (μM)	Cell lines	Diseases	References
6-1	60.0	A549	Non-small cell lung cancer	[75]
	63.9	HT-29	Colorectal Adenocarcinoma	
	53.4	MCF-7	Breast cancer	
	76.1	MDA-MB-231	Breast cancer	
6-2	22.67	A549	Non-small cell lung cancer	
	19.83	HT-29	Colorectal adenocarcinoma	
	23.81	MCF-7	Breast cancer	
	12.82	MDA-MB-231	Breast cancer	
6-3	10.38	A549	Non-small cell lung cancer	
	22.05	HT-29	Colorectal adenocarcinoma	
	9.93	MCF-7	Breast cancer	
	8.90	MDA-MB-231	Breast cancer	
	13.11	Vero E6 (African green monkey kidney epithelial cells)	/	
6-5	5.21	A549	Non-small cell lung cancer	
	27.74	HT-29	Colorectal adenocarcinoma	
	34.35	MCF-7	Breast cancer	
	19.20	MDA-MB-231	Breast cancer	
	> 100	Vero E6 (African green monkey kidney epithelial cells)	/	
6-6	36.12	A549	Non-small cell lung cancer	
	> 90	HT-29	Colorectal adenocarcinoma	
	47.84	MCF-7	Breast cancer	
	31.78	MDA-MB-231	Breast cancer	
	42.41	Vero E6 (African green monkey kidney epithelial cells)	/	
6-7	17.74	A549	Non-small cell lung cancer	
	26.16	HT-29	Colorectal adenocarcinoma	
	15.18	MCF-7	Breast cancer	
	15.18	MDA-MB-231	Breast cancer	
	22.23	Vero E6 (African green monkey kidney epithelial cells)	/	
6-8	17.93	A549	Non-small cell lung cancer	
	28.38	HT-29	Colorectal adenocarcinoma	
	14.63	MCF-7	Breast cancer	
	11.05	MDA-MB-231	Breast cancer	
	20.66	Vero E6 (African green monkey kidney epithelial cells)	/	
6-9	> 100	A549	Non-small cell lung cancer	
	> 100	HT-29	Colorectal adenocarcinoma	
	> 100	MCF-7	Breast cancer	
	> 100	MDA-MB-231	Breast cancer	
	> 100	Vero E6 (African green monkey kidney epithelial cells)	/	
6-10	3.35	A549	Non-small cell lung cancer	
	18.59	HT-29	Colorectal adenocarcinoma	
	20.00	MCF-7	Breast cancer	
	14.83	MDA-MB-231	Breast cancer	
	> 100	Vero E6 (African green monkey kidney epithelial cells)	/	
6-11	1.07	A549	Non-small cell lung cancer	
	5.78	HT-29	Colorectal adenocarcinoma	
	4.64	MCF-7	Breast cancer	
	2.51	MDA-MB-231	Breast cancer	
	31.54	Vero E6 (African green monkey kidney epithelial cells)	/	
6-12	0.89	A549	Non-small cell lung cancer	
	4.29	HT-29	Colorectal adenocarcinoma	
	3.91	MCF-7	Breast cancer	
	2.33	MDA-MB-231	Breast cancer	
	30.79	Vero E6 (African green monkey kidney epithelial cells)	/	
6-13	13.20 ± 1.70	OVCAR-8	Ovarian carcinoma	[76]
6-14	6.50 ± 0.10	OVCAR-8	Ovarian carcinoma	

clusters can also serve as radiosensitizers to enhance the killing effect on tumor cells during radiotherapy [86]. Figure 7 and Table 7 show the chemical structures and cytotoxicity of some some gold clusters.

3.1 Hypercarbon-centered organogold clusters

In 2022, Zhao et al. synthesized two hypercarbon-centered Au(I) cluster prodrugs, PAA4 and PAA5 (Fig. 7(a)). These two clusters maintained good stability in both phosphate buffered saline (PBS) and dulbecco's modified eagle's medium (DMEM). In *in vitro* experiments, researchers selected EJ cells for cytotoxicity assays. Results showed that both gold clusters exhibited high cytotoxicity, with IC_{50} values of 0.8 (PAA4) and 1.0 μM (PAA5), respectively. Further mechanism studies revealed that in human bladder cancer cells (EJ cells) with GSH overexpression and an acidic microenvironment, PAA4 could be triggered by GSH to release active Au(I). The released Au(I) efficiently inhibited TrxR, generated ROS, disrupted cellular redox balance, led to massive accumulation of lipid peroxides, and accelerated ferroptosis of EJ cells. There was also a significant inhibitory effect in mouse models of bladder cancer in situ, providing a new strategy for the development of metal prodrugs and the biological application of metal cluster compounds [87].

Subsequently, Zhao et al. also synthesized two hypercoordinate carbon-centered Au(I) clusters (HCGCs) [A5] and their dimer [A9] (Fig. 7(a)). [A9] possesses a symmetric [CAu_4-Au-CAu_4] structure. Compared with the structurally distorted [A5], it exhibited ultrafast intersystem crossing and a 0.41 μs triplet excited state with metal–metal-to-ligand charge-transfer characteristic. Under 560 nm light irradiation, [A9] could generate singlet oxygen ($^1O_2$) through a photodynamic process, oxidizing GSH in the cytoplasm to weakly coordinating GSSG, reducing the dissociation of [A9] in the cytoplasm and promoting its accumulation in mitochondria. The accumulation of [A9] in mitochondria reached 1.9 times that of the monomer [A5]. Subsequently, GSH further triggered the sustained release of active $[AuPPh_3]^+$, while inhibiting cytoplasmic glutathione

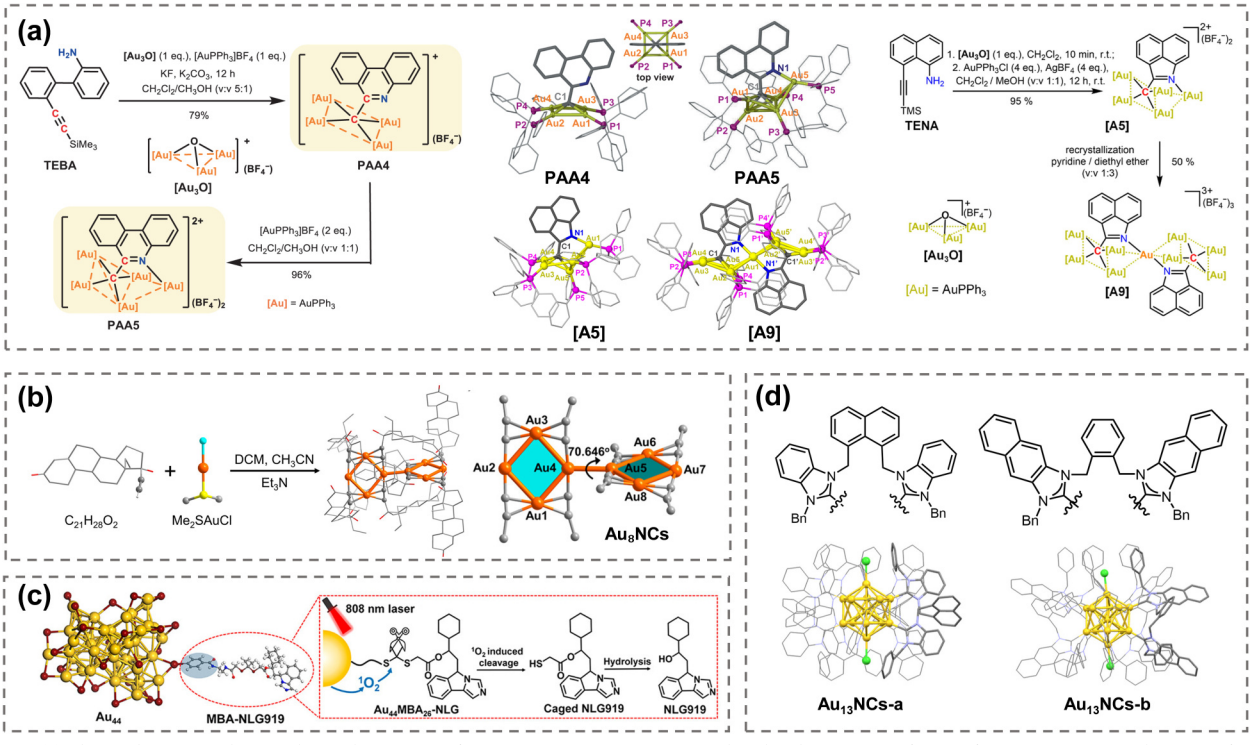

Figure 7 (a) The synthetic procedures and crystal structures of PAA4, PAA5, [A5], [A9]. Reproduced with permission from Ref. [87], © Xiao, K. et al. 2022; Ref. [88], © American Chemical Society 2025. (b) The synthetic procedures and crystal structures of Au_8NCs. Reproduced with permission from Ref. [90], © American Chemical Society 2019. (c) The crystal structures and working principle of the NIR photoactivation of Au44NCs. Reproduced with permission from Ref. [93], © American Chemical Society 2023. (d) The ligand structures and crystal structures of Au13NCs-a and Au13NCs-b. Reproduced with permission from Ref. [85], © American Chemical Society 2025.

Table 7 Cytotoxicity of some gold clusters

Clusters	IC_{50} (μM)	Cell lines	Diseases	References
PAA4	0.80	EJ	Bladder urothelial carcinoma	[87]
	2.10	HUVEC (human umbilical vein endothelial cells)	/	
PAA5	1.00	EJ	Bladder urothelial carcinoma	
	2.70	HUVEC (human umbilical vein endothelial cells)	/	
[A5]	2.15 (photocytotoxicity index)	EJ	Bladder urothelial carcinoma	[88]
[A9]	3.24 (photocytotoxicity index)	EJ	Bladder urothelial carcinoma	
Au_8NCs	7.80	EC1	Esophageal squamous cell carcinoma	[90]

peroxidase (GPX4) and TrxR2. This led to the ineffective scavenging of ROS and lipid peroxides, ultimately accelerating ferroptosis in EJ cells. This design provides a novel strategy for organometallic clusters with precise atomic structures to combat cancer via PDT [88].

3.2 Gold nanoclusters

In addition to the above mechanism for releasing mononuclear Au(I) species, the high atomic number of gold endows gold cluster drugs with the capacity to efficiently absorb X-rays and generate ROS for anticancer activity. For example, Zang et al. developed a radiosensitizer, gold-levonorgestrel nanoclusters (Au_8NCs) (Fig. 7(b)). With a size of approximately 2 nm, the nanoclusters possessed a high quantum yield of 58.7%. In *in vitro* experiments, compared with the group treated with X-rays alone, the combination of Au_8NCs and X-rays significantly reduced the survival fraction of human esophageal squamous cancer cells (EC1 cells). Mechanism studies revealed that Au_8NCs could generate a large amount of ROS under X-ray irradiation, leading to irreversible apoptosis of cancer cells. This study provided a new idea for the design of radiosensitizers at the atomic level [90].

Furthermore, AuNCs can also be used in PDT and PTT. For example, Crudden et al. reported two bisNHC-protected Au_{13} nanoclusters (Fig. 7(d)). These clusters are suitable for fluorescence imaging and PDT due to their high stability and high photoluminescence quantum yield (PLQY) [91]. By regulating the position of the π-expanded aromatic system on the bisNHC ligands, such as the linker or backbone of the bisNHC ligands, researchers found that enhanced ligand rigidity could improve PLQY (reaching 62% for 4a and 17% for 4b). The singlet oxygen quantum yield of Au_{13}NCs-a under light irradiation was 7.0% ± 0.9%, and the viability of human epithelial carcinoma cells (KB cells) decreased by 55% under 20 J/cm^2 of light treatment. Using KB tumor-bearing mice as models, real-time whole-body imaging and *ex vivo* fluorescence imaging demonstrated the potential of cluster Au_{13}NCs-a in tumor accumulation and fluorescence-based imaging applications [85].

Moreover, Yuan et al. developed a type of Au_{44}NCs. By conjugating with rigid aromatic Cy7 molecules (heptamethine dye), Au_{44}NCs exhibit strong NIR-II PL intensity, enable photoacoustic (PA) imaging, and achieve a high photothermal conversion efficiency of 65.12%. Furthermore, relying on the EPR effect, Au_{44}NCs can accumulate specifically at tumor sites. Under laser irradiation, these accumulated nanoclusters induce local hyperthermia to disrupt the structure of tumor cells, ultimately realizing efficient tumor ablation [92]. Subsequently, they conjugated Au_{44}NCs with the immune checkpoint inhibitor 1-cyclohexyl-2-(5H-imidazo[5,1-a]isoindol-5-yl)ethanol (NLG919), enabling the combined treatment of cancer via PDT/PTT and immunotherapy (Fig. 6(c)). This type of research provides a novel paradigm for non-invasive cancer treatment based on metal nanoclusters [93].

Different from gold coordination complexes, gold clusters contain more gold atoms, which endows them with exceptional optical properties. Therefore, gold clusters can not only act as chemotherapeutic agents but also be applied in PTT and PDT, as well as serve as radiosensitizers for radiotherapy. Meanwhile, with a size of less than 2 nm, gold clusters can cross biological barriers more readily. However, the synthesis of gold clusters requires stringent reaction conditions.

4 Conclusion and future outlook

Currently, gold-based drugs have exhibited potent anticancer activity and are regarded as promising next-generation metal-based anticancer agents following platinum-based drugs. This review mainly focuses on gold complexes, gold clusters with atomically defined structures, as well as their biological activities and mechanisms of action. Different from platinum-based drugs, due to the strong Au–S bond formation between Au and S, the most widely reported mechanism of action for gold-based drugs is the inhibition of TrxR activity. This disruption of intracellular redox homeostasis leads to increased levels of ROS, ultimately inducing cell death. However, how to efficiently deliver Au complexes and clusters to tumor sites while avoiding non-specific distribution remains a critical issue. It is still challenging to improve the stability and selectivity of drugs in complex biological environments and to prevent damage to normal tissues. Moreover, the specific targets of action and underlying chemical mechanisms of action for most Au complexes and clusters have not been fully elucidated. In addition, although gold clusters exhibit superior optical properties compared to gold complexes, the synthesis of gold cluster drugs with atomically defined structures is relatively challenging. At present, most research on gold-based drugs still focuses on simple gold complexes rather than gold clusters. It should be noted that gold nanoparticles without well-defined structures are not within the scope of this review.

We anticipate that the future advancement of Au complexes and clusters as anticancer drugs will still require continuous optimization of ligand structures. For instance, it is essential to develop superior chiral ligands to enable precise interaction with therapeutic targets, or introduce ligands with inherent pharmacological activity. Furthermore, the combination of multifunctional nanomaterials and targeted delivery systems represents a crucial strategy for enhancing the therapeutic efficacy of Au complexes and clusters. At the same time, it is necessary to ensure that Au complexes and clusters as anticancer drugs are effectively activated upon reaching the target, thereby exerting anticancer effects and improving the selectivity and specificity of the drugs. Au complexes and clusters as anticancer drugs should also be combined with other therapeutic approaches, such as immunotherapy, PDT, PTT, and radiation therapy. Finally, the mechanism of action of Au complexes and clusters as anticancer drugs *in vivo* also needs to be further studied in conjunction with techniques like electron microscopy to help us better understand the pharmacokinetics of the drugs.

Data availability

Not applicable.

Acknowledgements

Financial support by the National Natural Science Foundation of China (Nos. 22025105 and 22350002) and Fundamental and Interdisciplinary Disciplines Breakthrough Plan of the Ministry of Education of China (No. JYB2025XDXM413) is gratefully acknowledged.

Declaration of competing interest

All the contributing authors report no conflict of interests in this work.

Author contribution statement

X. N. A.: writing – original draft. L. Z.: Funding acquisition, supervision, writing – review & editing.

Use of AI statement

None.

References

[1] Rosenberg, B.; Vancamp, L.; Trosko, J. E.; Mansour, V. H. Platinum compounds: A new class of potent antitumour agents. *Nature* **1969**, *222*, 385–386.

[2] Brabec, V.; Hrabina, O.; Kasparkova, J. Cytotoxic platinum coordination compounds. DNA binding agents. *Coord. Chem. Rev.* **2017**, *351*, 2–31.

[3] Wang, D.; Lippard, S. J. Cellular processing of platinum anticancer drugs. *Nat. Rev. Drug Discov.* **2005**, *4*, 307–320.

[4] Yarbro, C. H. Carboplatin: A clinical review. *Semin. Oncol. Nurs.* **1989**, *5*, 63–69.

[5] Stein, A.; Arnold, D. Oxaliplatin: A review of approved uses. *Expert Opin. Pharmacother.* **2012**, *13*, 125–137.

[6] Kawai, Y.; Taniuchi, S.; Okahara, S.; Nakamura, M.; Gemba, M. Relationship between cisplatin or nedaplatin-induced nephrotoxicity and renal accumulation. *Biol. Pharm. Bull.* **2005**, *28*, 1385–1388.

[7] Eliopoulos, A. G.; Kerr, D. J.; Maurer, H. R.; Hilgard, P.; Spandidos, D. A. Induction of the c-*myc* but not the cH-*ras* promoter by platinum compounds. *Biochem. Pharmacol.* **1995**, *50*, 33–38.

[8] Kelland, L. The resurgence of platinum-based cancer chemotherapy. *Nat. Rev. Cancer.* **2007**, *7*, 573–584.

[9] Adhikari, S.; Nath, P.; Das, A.; Datta, A.; Baildya, N.; Duttaroy, A. K.; Pathak, S. A review on metal complexes and its anti-cancer activities: Recent updates from *in vivo* studies. *Biomed. Pharmacother.* **2024**, *171*, 116211.

[10] Cioroiu, C.; Weimer, L. H. Update on chemotherapy-induced peripheral neuropathy. *Curr. Neurol. Neurosci. Rep.* **2017**, *17*, 47.

[11] Padman, S.; Lee, J.; Kumar, R.; Slee, M.; Hakendorf, P.; Richards, A.; Koczwara, B.; Kichenadasse, G.; Sukumaran, S.; Roy, A. et al. Late effects of oxaliplatin-induced peripheral neuropathy (LEON)—cross-sectional cohort study of patients with colorectal cancer surviving at least 2 years. *Support. Care Cancer.* **2015**, *23*, 861–869.

[12] Zahednezhad, F.; Zakeri-Milani, P.; Shahbazi Mojarrad, J.; Valizadeh, H. The latest advances of cisplatin liposomal formulations: Essentials for preparation and analysis. *Expert Opin. Drug Deliv.* **2020**, *17*, 523–541.

[13] Štarha, P.; Křikavová, R. Platinum(IV) and platinum(II) anticancer complexes with biologically active releasable ligands. *Coord. Chem. Rev.* **2024**, *501*, 215578.

[14] Ott, I.; Gust, R. Non platinum metal complexes as anti-cancer drugs. *Arch. Pharm.* **2007**, *340*, 117–126.

[15] Mjos, K. D.; Orvig, C. Metallodrugs in medicinal inorganic chemistry. *Chem. Rev.* **2014**, *114*, 4540–4563.

[16] Ott, I. On the medicinal chemistry of gold complexes as anticancer drugs. *Coord. Chem. Rev.* **2009**, *253*, 1670–1681.

[17] Lu, Y. L.; Ma, X. Y.; Chang, X. Y.; Liang, Z. L.; Lv, L.; Shan, M.; Lu, Q. Y.; Wen, Z. F.; Gust, R.; Liu, W. K. Recent development of gold(i) and gold(iii) complexes as therapeutic agents for cancer diseases. *Chem. Soc. Rev.* **2022**, *51*, 5518–5556.

[18] Huaizhi, Z.; Yuantao, N. China's ancient gold drugs. *Gold Bull.* **2001**, *34*, 24–29.

[19] Kean, W. F.; Forestier, F.; Kassam, Y.; Buchanan, W. W.; Rooney, P. J. The history of gold therapy in rheumatoid disease. *Semin. Arthritis Rheum.* **1985**, *14*, 180–186.

[20] Sutton, B. M.; McGusty, E.; Walz, D. T.; DiMartino, M. J. Oral gold. Antiarthritic properties of alkylphosphinegold coordination complexes. *J. Med. Chem.* **1972**, *15*, 1095–1098.

[21] Finkelstein, A. E.; Walz, D. T.; Batista, V.; Mizraji, M.; Roisman, F.; Misher, A. Auranofin. New oral gold compound for treatment of rheumatoid arthritis. *Ann. Rheum. Dis.* **1976**, *35*, 251–257.

[22] Roder, C.; Thomson, M. J. Auranofin: Repurposing an old drug for a golden new age. *Drugs R D* **2015**, *15*, 13–20.

[23] Rothan, H. A.; Stone, S.; Natekar, J.; Kumari, P.; Arora, K.; Kumar, M. The FDA-approved gold drug auranofin inhibits novel coronavirus (SARS-COV-2) replication and attenuates inflammation in human cells. *Virology* **2020**, *547*, 7–11.

[24] Capparelli, E. V.; Bricker-Ford, R.; Rogers, M. J.; McKerrow, J. H.; Reed, S. L. Phase I clinical trial results of auranofin, a novel antiparasitic agent. *Antimicrob. Agents Chemother.* **2017**, *61*, e01947–16.

[25] Wang, H.; Bouzakoura, S.; De Mey, S.; Jiang, H.; Law, K.; Dufait, I.; Corbet, C.; Verovski, V.; Gevaert, T.; Feron, O. et al. Auranofin radiosensitizes tumor cells through targeting thioredoxin reductase and resulting overproduction of reactive oxygen species. *Oncotarget* **2017**, *8*, 35728–35742.

[26] Marzano, C.; Gandin, V.; Folda, A.; Scutari, G.; Bindoli, A.; Rigobello, M. P. Inhibition of thioredoxin reductase by auranofin induces apoptosis in cisplatin-resistant human ovarian cancer cells. *Free Radical Biol. Med.* **2007**, *42*, 872–881.

[27] Rigobello, M. P.; Gandin, V.; Folda, A.; Rundlöf, A. K.; Fernandes, A. P.; Bindoli, A.; Marzano, C.; Björnstedt, M. Treatment of human cancer cells with selenite or tellurite in combination with auranofin enhances cell death due to redox shift. *Free Radical Biol. Med.* **2009**, *47*, 710–721.

[28] McKeage, M. J.; Maharaj, L.; Berners-Price, S. J. Mechanisms of cytotoxicity and antitumor activity of gold(I) phosphine complexes: The possible role of mitochondria. *Coord. Chem. Rev.* **2002**, *232*, 127–135.

[29] Brown, K. K.; Cox, A. G.; Hampton, M. B. Mitochondrial respiratory chain involvement in peroxiredoxin 3 oxidation by phenethyl isothiocyanate and auranofin. *FEBS Lett.* **2010**, *584*, 1257–1262.

[30] Onodera, T.; Momose, I.; Kawada, M. Potential anticancer activity of auranofin. *Chem. Pharm. Bull.* **2019**, *67*, 186–191.

[31] Yamashita, M. Auranofin: Past to present, and repurposing. *Int. Immunopharmacol.* **2021**, *101*, 108272.

[32] Park, S. J.; Kim, I. S. The role of p38 MAPK activation in auranofin-induced apoptosis of human promyelocytic leukaemia HL-60 cells. *Br. J. Pharmacol.* **2005**, *146*, 506–513.

[33] Newman, Z. L.; Sirianni, N.; Mawhinney, C.; Lee, M. S.; Leppla, S. H.; Moayeri, M.; Johansen, L. M. Auranofin protects against anthrax lethal toxin-induced activation of the Nlrp1b inflammasome. *Antimicrob. Agents Chemother.* **2011**, *55*, 1028–1035.

[34] Madeira, J. M.; Gibson, D. L.; Kean, W. F.; Klegeris, A. The biological activity of auranofin: Implications for novel treatment of diseases. *Inflammopharmacology* **2012**, *20*, 297–306.

[35] Sze, J. H.; Raninga, P. V.; Nakamura, K.; Casey, M.; Khanna, K. K.; Berners-Price, S. J.; Di Trapani, G.; Tonissen, K. F. Anticancer activity of a Gold(I) phosphine thioredoxin reductase inhibitor in multiple myeloma. *Redox Biol.* **2020**, *28*, 101310.

[36] Rackham, O.; Nichols, S. J.; Leedman, P. J.; Berners-Price, S. J.; Filipovska, A. A gold(I) phosphine complex selectively induces apoptosis in breast cancer cells: Implications for anticancer therapeutics targeted to mitochondria. *Biochem. Pharmacol.* **2007**, *74*, 992–1002.

[37] Marzo, T.; Cirri, D.; Gabbiani, C.; Gamberi, T.; Magherini, F.; Pratesi, A.; Guerri, A.; Biver, T.; Binacchi, F.; Stefanini, M. et al. Auranofin, Et_3PAuCl, and Et_3PAuI are highly cytotoxic on colorectal cancer cells: A chemical and biological study. *ACS Med. Chem. Lett.* **2017**, *8*, 997–1001.

[38] Bindoli, A.; Rigobello, M. P.; Scutari, G.; Gabbiani, C.; Casini, A.;

Messori, L. Thioredoxin reductase: A target for gold compounds acting as potential anticancer drugs. *Coord. Chem. Rev.* **2009**, *253*, 1692–1707.
[39] Zhao, Q.; Han, B.; Peng, C.; Zhang, N.; Huang, W.; He, G.; Li, J. L. A promising future of metal-N-heterocyclic carbene complexes in medicinal chemistry: The emerging bioorganometallic antitumor agents. *Med. Res. Rev.* **2024**, *44*, 2194–2235.
[40] Storr, T.; Thompson, K. H.; Orvig, C. Design of targeting ligands in medicinal inorganic chemistry. *Chem. Soc. Rev.* **2006**, *35*, 534–544.
[41] Mirzadeh, N.; Reddy, T. S.; Bhargava, S. K. Advances in diphosphine ligand-containing gold complexes as anticancer agents. *Coord. Chem. Rev.* **2019**, *388*, 343–359.
[42] Shen, S. Y.; Shen, J.; Luo, Z.; Wang, F. D.; Min, J. X. Molecular mechanisms and clinical implications of the gold drug auranofin. *Coord. Chem. Rev.* **2023**, *493*, 215323.
[43] Schmidt, C.; Albrecht, L.; Balasupramaniam, S.; Misgeld, R.; Karge, B.; Brönstrup, M.; Prokop, A.; Baumann, K.; Reichl, S.; Ott, I. A gold(I) biscarbene complex with improved activity as a TrxR inhibitor and cytotoxic drug: Comparative studies with different gold metallodrugs. *Metallomics* **2019**, *11*, 533–545.
[44] Guo, W. J.; Peng, T. K.; Zhu, W. P.; Ma, S. X.; Wang, G.; Li, Y.; Liu, B.; Peng, H. Q. Visualization of supramolecular assembly by aggregation-induced emission. *Aggregate* **2023**, *4*, e297.
[45] Ye, Z. Y.; He, W.; Zhang, Z. C.; Qiu, Z. J.; Zhao, Z.; Tang, B. Z. AIEgens for microorganism-related visualization and therapy. *Interdiscip. Med.* **2023**, *1*, e20220011.
[46] Feng, N.; Peng, Z.; Zhang, X.; Lin, Y. L.; Hu, L. R.; Zheng, L.; Tang, B. Z.; Zhang, J. Strategically engineered Au(I) complexes for orchestrated tumor eradication via chemo-phototherapy and induced immunogenic cell death. *Nat. Commun.* **2024**, *15*, 8187.
[47] Hopkinson, M. N.; Richter, C.; Schedler, M.; Glorius, F. An overview of N-heterocyclic carbenes. *Nature* **2014**, *510*, 485–496.
[48] Barnard, P. J.; Baker, M. V.; Berners-Price, S. J.; Day, D. A. Mitochondrial permeability transition induced by dinuclear gold(I)-carbene complexes: Potential new antimitochondrial antitumour agents. *J. Inorg. Biochem.* **2004**, *98*, 1642–1647.
[49] Fritz-Wolf, K.; Urig, S.; Becker, K. The structure of human thioredoxin reductase 1 provides insights into C-terminal rearrangements during catalysis. *J. Mol. Biol.* **2007**, *370*, 116–127.
[50] Liu, W. K.; Bensdorf, K.; Proetto, M.; Abram, U.; Hagenbach, A.; Gust, R. NHC gold halide complexes derived from 4, 5-diarylimidazoles: Synthesis, structural analysis, and pharmacological investigations as potential antitumor agents. *J. Med. Chem.* **2011**, *54*, 8605–8615.
[51] Bian, M. L.; Fan, R.; Jiang, G. Z.; Wang, Y. X.; Lu, Y. L.; Liu, W. K. Halo and pseudohalo gold(I)-NHC complexes derived from 4, 5-diarylimidazoles with excellent *in vitro* and *in vivo* anticancer activities against HCC. *J. Med. Chem.* **2020**, *63*, 9197–9211.
[52] Hickey, J. L.; Ruhayel, R. A.; Barnard, P. J.; Baker, M. V.; Berners-Price, S. J.; Filipovska, A. Mitochondria-targeted chemotherapeutics: The rational design of gold(I) *N*-heterocyclic carbene complexes that are selectively toxic to cancer cells and target protein selenols in preference to thiols. *J. Am. Chem. Soc.* **2008**, *130*, 12570–12571.
[53] Baker, M. V.; Barnard, P. J.; Berners-Price, S. J.; Brayshaw, S. K.; Hickey, J. L.; Skelton, B. W.; White, A. H. Cationic, linear Au(i) *N*-heterocyclic carbene complexes: Synthesis, structure and anti-mitochondrial activity. *Dalton Trans*. **2006**, 3708–3715.
[54] Bannwart, F.; Richter, L. F.; Stifel, S.; Rueter, J.; Lode, H. N.; Correia, J. D. G.; Kühn, F. E.; Prokop, A. A New class of gold(I) NHC complexes with proapoptotic and resensitizing properties towards multidrug resistant leukemia cells overexpressing BCL-2. *J. Med. Chem.* **2024**, *67*, 15494–15508.
[55] Long, Y.; Cao, B.; Xiong, X. L.; Chan, A. S. C.; Sun, R. W. Y.; Zou, T. T. Bioorthogonal activation of dual catalytic and anti-cancer activities of organogold(I) complexes in living systems. *Angew. Chem., Int. Ed.* **2021**, *60*, 4133–4141.
[56] Wang, Y.; Du, H. L.; Zhai, G. X. Recent advances in active hepatic targeting drug delivery system. *Curr. Drug Targets* **2014**, *15*, 573–599.
[57] Yang, Z. B.; Bian, M. L.; Lv, L.; Chang, X. Y.; Wen, Z. F.; Li, F. W.; Lu, Y. L.; Liu, W. K. Tumor-targeting NHC-Au(I) complex induces immunogenic cell death in hepatocellular carcinoma. *J. Med. Chem.* **2023**, *66*, 3934–3952.
[58] Lu, Y. L.; Sheng, X. Y.; Liu, C.; Liang, Z. L.; Wang, X.; Liu, L. J.; Wen, Z. F.; Yang, Z. B.; Du, Q. M.; Liu, W. K. SERD-NHC-Au(I) complexes for dual targeting ER and TrxR to induce ICD in breast cancer. *Pharmacol. Res.* **2023**, *190*, 106731.
[59] Lacoma, T.; Forté, J.; Maruchenko, R.; Morichon, R.; Salmain, M.; Sobczak-Thépot, J.; Bertrand, B. Impact of chelation on reactivity and cytotoxicity of hemilabile biphenyl gold(III) N-heterocyclic carbene complexes. *ChemMedChem* **2025**, *20*, e202500302.
[60] Bohan, P. T.; Toste, F. D. Well-defined chiral gold(III) complex catalyzed direct enantioconvergent kinetic resolution of 1, 5-enynes. *J. Am. Chem. Soc.* **2017**, *139*, 11016–11019.
[61] Jouhannet, R.; Dagorne, S.; Blanc, A.; De Frémont, P. Chiral gold(III) complexes: Synthesis, structure, and potential applications. *Chem.—Eur. J.* **2021**, *27*, 9218–9240.
[62] Arojojoye, A. S.; Kim, J. H.; Olelewe, C.; Parkin, S.; Awuah, S. G. Chiral gold(iii) complexes: Speciation, *in vitro*, and *in vivo* anticancer profile. *Chem. Commun.* **2022**, *58*, 10237–10240.
[63] Estrada-Ortiz, N.; Guarra, F.; De Graaf, I. A. M.; Marchetti, L.; De Jager, M. H.; Groothuis, G. M. M.; Gabbiani, C.; Casini, A. Anticancer gold *N*-heterocyclic carbene complexes: A comparative *in vitro* and ex vivo study. *ChemMedChem* **2017**, *12*, 1429–1435.
[64] Messori, L.; Marchetti, L.; Massai, L.; Scaletti, F.; Guerri, A.; Landini, I.; Nobili, S.; Perrone, G.; Mini, E.; Leoni, P. et al. Chemistry and biology of two novel gold(I) carbene complexes as prospective anticancer agents. *Inorg. Chem.* **2014**, *53*, 2396–2403.
[65] Guarra, F.; Terenzi, A.; Pirker, C.; Passannante, R.; Baier, D.; Zangrando, E.; Gómez-Vallejo, V.; Biver, T.; Gabbiani, C.; Berger, W. et al. ^{124}I radiolabeling of a Au^{III}-NHC complex for *in vivo* biodistribution studies. *Angew. Chem., Int. Ed.* **2020**, *59*, 17130–17136.
[66] Reddy, T. S.; Privér, S. H.; Mirzadeh, N.; Bhargava, S. K. Anti-cancer gold(I) phosphine complexes: Cyclic trimers and tetramers containing the P–Au–P moiety. *J. Inorg. Biochem.* **2017**, *175*, 1–8.
[67] Movassaghi, S.; Singh, S.; Mansur, A.; Tong, K. K. H.; Hanif, M.; Holtkamp, H. U.; Söhnel, T.; Jamieson, S. M. F.; Hartinger, C. G. (Pyridin-2-yl)-NHC organoruthenium complexes: Antiproliferative properties and reactivity toward biomolecules. *Organometallics* **2018**, *37*, 1575–1584.
[68] Kim, J. H.; Ofori, S.; Parkin, S.; Vekaria, H.; Sullivan, P. G.; Awuah, S. G. Anticancer gold(iii)-bisphosphine complex alters the mitochondrial electron transport chain to induce *in vivo* tumor inhibition. *Chem. Sci.* **2021**, *12*, 7467–7479.
[69] Fleischer, E. B.; Laszlo, A. Synthesis of a gold porphyrin. *Inorg. Nucl. Chem. Lett.* **1969**, *5*, 373–376.
[70] Che, C. M.; Sun, R. W. Y.; Yu, W. Y.; Ko, C. B.; Zhu, N. Y.; Sun, H. Z. Gold(iii) porphyrins as a new class of anticancer drugs: Cytotoxicity, DNA binding and induction of apoptosis in human cervix epitheloid cancer cells. *Chem. Commun*. **2003**, 1718–1719.
[71] Fan, W. P.; Huang, P.; Chen, X. Y. Overcoming the Achilles' heel of photodynamic therapy. *Chem. Soc. Rev.* **2016**, *45*, 6488–6519.
[72] Toubia, I.; Nguyen, C.; Diring, S.; Ali, L. M. A.; Larue, L.; Aoun, R.; Frochot, C.; Gary-Bobo, M.; Kobeissi, M.; Odobel, F. Synthesis and anticancer activity of gold porphyrin linked to malonate diamine platinum complexes. *Inorg. Chem.* **2019**, *58*, 12395–12406.
[73] Bian, M. L.; Wang, X.; Sun, Y.; Liu, W. K. Synthesis and biological evaluation of gold(III) Schiff base complexes for the treatment of hepatocellular carcinoma through attenuating TrxR activity. *Eur. J.*

Med. Chem. **2020**, *193*, 112234.
[74] Mahdavi, S. M.; Bockfeld, D.; Büssing, R.; Karge, B.; Bannenberg, T.; Frank, R.; Brönstrup, M.; Ott, I.; Tamm, M. Synthesis of N-heterocyclic carbene gold(i) complexes from the marine betaine 1, 3-dimethylimidazolium-4-carboxylate. *Dalton Trans.* **2024**, *53*, 1942–1946.
[75] Mahdavi, S. M.; Bockfeld, D.; Esarev, I. V.; Lippmann, P.; Frank, R.; Brönstrup, M.; Ott, I.; Tamm, M. Gold(i) and gold(iii) carbene complexes from the marine betaine norzooanemonin: Inhibition of thioredoxin reductase, antiproliferative and antimicrobial activity. *RSC Med. Chem.* **2024**, *15*, 3248–3255.
[76] Al-Buthabhak, H. S.; Al-Ameed, K.; Yu, Y.; Sobolev, A. N.; Moggach, S. A.; Al-Salami, H.; Ferro, V.; Baker, M. V. Gold(i) and gold(iii) complexes of triazolyl-functionalised NHCs. *RSC Adv.* **2025**, *15*, 18123–18141.
[77] Singh, P.; Joshi, A. S.; Singh, H.; Mijakovic, I. Medical importance and pharmacokinetics of gold nanoparticles in the human body. *Mol. Cancer* **2025**, *24*, 252.
[78] Huang, X. H.; Jain, P. K.; El-Sayed, I. H.; El-Sayed, M. A. Plasmonic photothermal therapy (PPTT) using gold nanoparticles. *Lasers Med. Sci.* **2008**, *23*, 217–228.
[79] Turkmen Koc, S. N.; Rezaei Benam, S.; Aral, I. P.; Shahbazi, R.; Ulubayram, K. Gold nanoparticles-mediated photothermal and photodynamic therapies for cancer. *Int. J. Pharm.* **2024**, *655*, 124057.
[80] Zhang, B. H.; Liu, Z. H.; Zhang, R. X.; Yao, Q. F.; Xie, J. P. Precision metal nanoclusters meet proteins: Crafting next-gen hybrid materials. *ACS Nano* **2025**, *19*, 3997–4010.
[81] Xiao, F.; Chen, Y.; Qi, J.; Yao, Q. F.; Xie, J. P.; Jiang, X. Y. Multi-targeted peptide-modified gold nanoclusters for treating solid tumors in the liver. *Adv. Mater.* **2023**, *35*, e2210412.
[82] Zhang, X. D.; Wu, D.; Shen, X.; Liu, P. X.; Fan, F. Y.; Fan, S. J. *In vivo* renal clearance, biodistribution, toxicity of gold nanoclusters. *Biomaterials* **2012**, *33*, 4628–4638.
[83] Sharma, N.; Mohammad, W.; Le Guével, X.; Shanavas, A. Gold nanoclusters as high resolution NIR-II theranostic agents. *Chem. Biomed. Imaging* **2024**, *2*, 462–480.
[84] Yang, K.; Zhao, S. J.; Li, B. L.; Wang, B. H.; Lan, M. H.; Song, X. Z. Low temperature photothermal therapy: Advances and perspectives. *Coord. Chem. Rev.* **2022**, *454*, 214330.
[85] Kulkarni, V. K.; Albright, E. L.; Zeinizade, E.; Steele, E.; Chen, J.; Ding, L. L.; Malola, S.; Takano, S.; Harrington, K.; Kwon, N. et al. Impact of ligand structure on biological activity and photophysical properties of NHC-protected Au_{13} nanoclusters. *J. Am. Chem. Soc.* **2025**, *147*, 4017–4025.
[86] Hua, Y.; Shao, Z. H.; Zhai, A. Q.; Zhang, L. J.; Wang, Z. Y.; Zhao, G.; Xie, F. W.; Liu, J. Q.; Zhao, X. L.; Chen, X. Y. et al. Water-soluble Au_{25} clusters with single-crystal structure for mitochondria-targeting radioimmunotherapy. *ACS Nano* **2023**, *17*, 7837–7846.
[87] Xiao, K.; Zhang, N. Y.; Li, F. F.; Hou, D. Y.; Zhai, X. Y.; Xu, W. H.; Wang, G. L.; Wang, H.; Zhao, L. Pro-oxidant response and accelerated ferroptosis caused by synergetic Au(I) release in hypercarbon-centered gold(I) cluster prodrugs. *Nat. Commun.* **2022**, *13*, 4669.
[88] Xiao, K.; Hou, D. Y.; Zhang, N. Y.; Wang, W.; Leung, M. Y.; Kwok, W. K.; Chen, Z. Y.; Jin, C.; Xu, W. H.; Wang, H. et al. Synergistic enhancement of ferroptosis via mitochondrial accumulation and photodynamic-controlled release of an organogold(I) cluster prodrug. *J. Am. Chem. Soc.* **2025**, *147*, 4482–4492.
[89] Bourehil, L.; Soep, C.; Seng, S.; Dutrannoy, S.; Igoudjil, S.; Forté, J.; Gontard, G.; Lesage, D.; Bertrand, B.; Dossmann, H. Bond-dissociation energies to probe pyridine electronic effects on organogold(III) complexes: From methodological developments to application in π-backdonation investigation and catalysis. *Inorg. Chem.* **2023**, *62*, 13304–13314.
[90] Jia, T. T.; Yang, G.; Mo, S. J.; Wang, Z. Y.; Li, B. J.; Ma, W.; Guo, Y. X.; Chen, X. Y.; Zhao, X. L.; Liu, J. Q. et al. Atomically precise gold-levonorgestrel nanocluster as a radiosensitizer for enhanced cancer therapy. *ACS Nano* **2019**, *13*, 8320–8328.
[91] Shen, H.; Xiang, S. J.; Xu, Z.; Liu, C.; Li, X. H.; Sun, C. F.; Lin, S. C.; Teo, B. K.; Zheng, N. F. Superatomic Au_{13} clusters ligated by different N-heterocyclic carbenes and their ligand-dependent catalysis, photoluminescence, and proton sensitivity. *Nano Res.* **2020**, *13*, 1908–1911.
[92] Yang, G.; Mu, X.; Pan, X. X.; Tang, Y.; Yao, Q. F.; Wang, Y. R.; Jiang, F. Y.; Du, F. L.; Xie, J. P.; Zhou, X. F. et al. Ligand engineering of Au_{44} nanoclusters for NIR-II luminescent and photoacoustic imaging-guided cancer photothermal therapy. *Chem. Sci.* **2023**, *14*, 4308–4318.
[93] Yang, G.; Pan, X. X.; Feng, W. B.; Yao, Q. F.; Jiang, F. Y.; Du, F. L.; Zhou, X. F.; Xie, J. P.; Yuan, X. Engineering Au_{44} Nanoclusters for NIR-II Luminescence Imaging-Guided Photoactivatable Cancer Immunotherapy. *ACS Nano* **2023**, *17*, 15605–15614.